Journal of Applied Mechanics and Technical Physics, Vol. 51, No. 2, pp. 182–192, 2010

NUMERICAL MODELING OF INTERACTION BETWEEN A TURBULENT MIXING ZONE AND A LOCAL PERTURBATION OF THE DENSITY FIELD IN A PYCNOCLINE

O. F. Voropayeva and G. G. Chernykh

UDC 532.517.4

A numerical model is developed, and interaction between a turbulent mixing zone and a local perturbation of the density field in a pycnocline is studied. It is demonstrated that the flow induced by a local perturbation of the density field can generate turbulence energy in the turbulent mixing zone and increase its lifetime.

Key words: *turbulent mixing zone, local perturbation of the density field, pycnocline, modified $e-\varepsilon$ turbulence model, numerical modeling.*

Introduction. The problem of the dynamics of localized turbulent structures (turbulent mixing zones or turbulent spots) in a stable stratified medium is well known [1, 2]. Turbulent spots exert a significant effect on the formation of a thin-layer vertical microstructure of flows in the ocean [2]. A plane model problem of the evolution of the turbulent mixing zone in a linearly stratified medium was considered in [3], where a mathematical model of the flow including the equation of the turbulence energy balance was constructed and calculated results were presented. It follows from those results that expansion of the turbulent mixing zone occurs at the initial stage under the action of turbulent diffusion, followed by the vertical collapse of this zone owing to the gravity force. It was shown that the evolution of the turbulent mixing zone is accompanied by intense generation of internal waves. Vasiliev et al. [4] studied the flow on the basis of the numerical model with differential transport equations for the normal Reynolds stresses. Kao and Pao [5] demonstrated in their experiments on the evolution of the turbulent mixing zone in a pycnocline that soliton-type internal waves can be generated in the flow. The dynamics of the turbulent mixing zone in a fluid with stable nonlinear stratification was numerically modeled in [6]. Investigations of the evolution of plane turbulent spots in stratified media were reviewed in detail in [7, 8]. This problem without turbulent perturbations is known as the problem of the dynamics of a local perturbation of the density field in a stable stratified medium (see, e.g., [3, 6, 9–12] and references therein). Interaction of two laminar spots of a completely mixed fluid in a linearly stratified medium was experimentally studied in [13]. An experimental study of interaction of two regions of a mixed fluid in a pycnocline was performed in [14].

An analysis of publications on this topic shows that there are fairly effective numerical models that describe the dynamics of individual local zones of turbulent and laminar mixing in a pycnocline. At the same time, there are practically no investigations in the field of mathematical modeling of interaction of these flows. In the present work, this problem is solved on the basis of a modified $e-\varepsilon$ turbulence model.

Institute of Computational Technologies, Siberian Division, Russian Academy of Sciences, Novosibirsk 630090. Novosibirsk State University, Novosibirsk 630090; vorop@ict.nsc.ru; chernykh@ict.nsc.ru. Translated from Prikladnaya Mekhanika i Tekhnicheskaya Fizika, Vol. 51, No. 2, pp. 49–60, March–April, 2010. Original article submitted April 17, 2009.

1. Formulation of the Problem. The flow is described by a system of the averaged equations of hydrodynamics in the Oberbeck–Boussinesq approximation

$$\begin{gathered}
\frac{\partial U}{\partial t}+U\,\frac{\partial U}{\partial x}+V\,\frac{\partial U}{\partial y}=-\frac{1}{\rho_0}\,\frac{\partial\langle p_1\rangle}{\partial x}-\frac{\partial}{\partial x}\,\langle u'^2\rangle-\frac{\partial}{\partial y}\,\langle u'v'\rangle,\\
\frac{\partial V}{\partial t}+U\,\frac{\partial V}{\partial x}+V\,\frac{\partial V}{\partial y}=-\frac{1}{\rho_0}\,\frac{\partial\langle p_1\rangle}{\partial y}-\frac{\partial}{\partial x}\,\langle u'v'\rangle-\frac{\partial}{\partial y}\,\langle v'^2\rangle-g\,\frac{\langle\rho_1\rangle}{\rho_0},\\
\frac{\partial\langle\rho_1\rangle}{\partial t}+U\,\frac{\partial\langle\rho_1\rangle}{\partial x}+V\,\frac{\partial\langle\rho_1\rangle}{\partial y}+V\,\frac{d\rho_s}{dy}=-\frac{\partial}{\partial x}\,\langle u'\rho'\rangle-\frac{\partial}{\partial y}\,\langle v'\rho'\rangle,\\
\frac{\partial U}{\partial x}+\frac{\partial V}{\partial y}=0,
\end{gathered}\tag{1}$$

where $u'=u'_1$ and $v'=u'_2$ are the fluctuating components of velocity in the directions of the axes $x=x_1$ and $y=x_2$, respectively, $U=U_1$ and $V=U_2$ are the components of velocity of averaged motion, $\boldsymbol{g}=(0,-g)$, where g is the gravity acceleration, $\rho_s=\rho_s(y)$ is the density of the unperturbed stable stratified fluid, $\rho_0=\rho_s(0)$, $\langle\rho_1\rangle=\langle\rho\rangle-\rho_s$ is the averaged defect of density, $\langle\rho\rangle$ is the averaged density, and p_1 is the deviation of pressure from the hydrostatic value due to stratification; the broken brackets mean the averaging operation.

System (1) is nonclosed. To close this system, we use a modified e–ε turbulence model based on the transport equations for the turbulence energy e, dissipation rate ε, and tangential component of the Reynolds stress tensor $\langle u'v'\rangle$, and also the algebraic presentations of the normal ($i=j=1,2$) components of the Reynolds stress tensor $\langle u'_iu'_j\rangle$, components of the turbulent flux vector $\langle u'_i\rho'\rangle$, and dispersion of density field fluctuations $\langle\rho'^2\rangle$ [6, 8, 15]:

$$\begin{gathered}
\frac{\partial e}{\partial t}+U_k\,\frac{\partial e}{\partial x_k}=\frac{\partial}{\partial x_k}\Big(c_s\,\frac{e}{\varepsilon}\,\langle u'_ku'_k\rangle\,\frac{\partial e}{\partial x_k}\Big)+P-\varepsilon,\\
\frac{\partial\varepsilon}{\partial t}+U_k\,\frac{\partial\varepsilon}{\partial x_k}=\frac{\partial}{\partial x_k}\Big(\frac{c_s}{\sigma}\,\frac{e}{\varepsilon}\,\langle u'_ku'_k\rangle\,\frac{\partial\varepsilon}{\partial x_k}\Big)+c_{\varepsilon1}\,\frac{\varepsilon}{e}\,P-c_{\varepsilon2}\,\frac{\varepsilon^2}{e},\\
\frac{\partial\langle u'v'\rangle}{\partial t}+U_k\,\frac{\partial\langle u'v'\rangle}{\partial x_k}=\frac{\partial}{\partial x_k}\Big(c_s\,\frac{e}{\varepsilon}\,\langle u'_ku'_k\rangle\,\frac{\partial\langle u'v'\rangle}{\partial x_k}\Big)+(1-c_2)P_{12}-c_1\,\frac{\varepsilon}{e}\,\langle u'v'\rangle,\\
\frac{\langle u'_iu'_j\rangle}{e}=\frac{2}{3}\,\delta_{ij}+\frac{1-c_2}{c_1}\Big(\frac{P_{ij}}{\varepsilon}+\frac{2}{3}\,\delta_{ij}\,\frac{P}{\varepsilon}\Big),\\
-\langle u'_i\rho'\rangle=\frac{e}{c_{1T}\varepsilon}\Big(\langle u'^2_i\rangle\,\frac{\partial\langle\rho\rangle}{\partial x_i}-(1-c_{2T})\,\frac{g_i}{\rho_0}\,\langle\rho'^2\rangle\Big),\\
\langle\rho'^2\rangle=-\frac{2}{c_T}\,\frac{e}{\varepsilon}\,\langle v'\rho'\rangle\,\frac{\partial\langle\rho\rangle}{\partial y}\qquad(k=1,2).
\end{gathered}$$

Here δ_{ij} is the Kronecker delta and $c_1=2.2$, $c_2=0.55$, $c_{1T}=3.2$, $c_{2T}=0.5$, $c_T=1.25$, $c_{\varepsilon1}=1.45$, $c_{\varepsilon2}=1.92$, $c_s=0.25$, and $\sigma=1.3$ are empirical constants [15]; summation is performed over the repeated index k. The terms that describe energy generation due to averaged motion and the action of the gravity force are defined in a standard manner:

$$P_{ij}=-\Big(\langle u'_iu'_k\rangle\,\frac{\partial U_j}{\partial x_k}+\langle u'_ju'_k\rangle\,\frac{\partial U_i}{\partial x_k}-\frac{g_i}{\rho_0}\,\langle u'_j\rho'\rangle-\frac{g_j}{\rho_0}\,\langle u'_i\rho'\rangle\Big),\qquad P=\frac{P_{kk}}{2}.$$

The initial and boundary conditions are

$$\begin{gathered}
U=V=\langle\rho_1\rangle=\langle u'v'\rangle=0,\quad\varepsilon=\varepsilon_0(r),\quad e=e_0(r),\quad t=0,\quad r^2=x^2+y^2,\\
U=V=\langle\rho_1\rangle=\langle u'v'\rangle=\varepsilon=e=0,\qquad r\to\infty,\quad t>0.
\end{gathered}\tag{2}$$

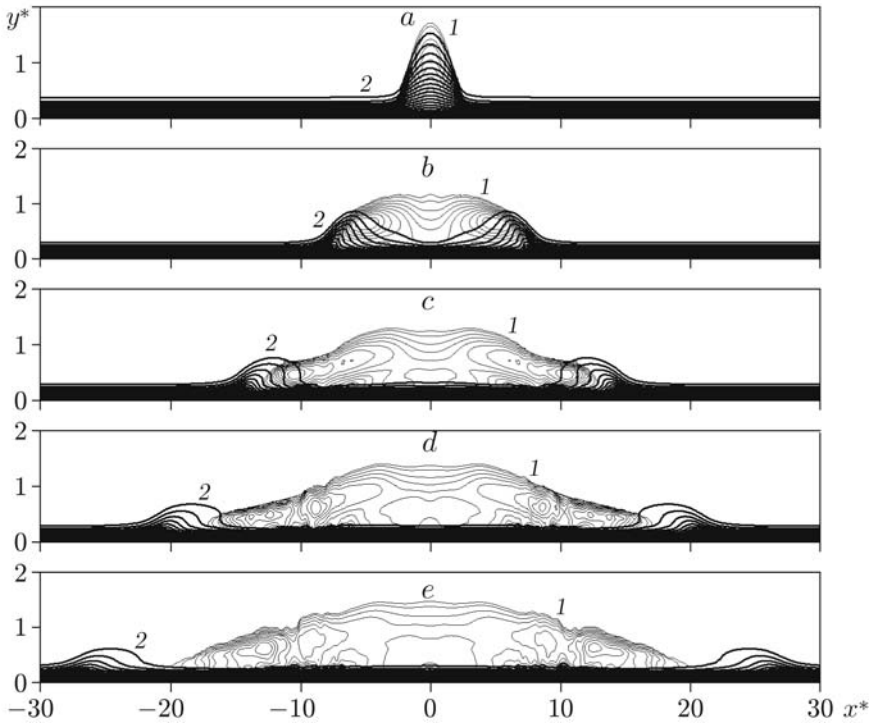

Fig. 1. Contours of the turbulence energy (1) and averaged density (2) in the problem of the dynamics of a single region of turbulent perturbations in a pycnocline at different times: $t/T = 1$ (a), 5 (b), 10 (c), 15 (d), and 20 (e).

The laminar local perturbation of the density field with the center at the point $x = x_0$ at $t = 0$ is defined in the form

$$\langle \rho_1 \rangle = (\rho_0 - \rho_s)\delta \exp\left(-(\alpha r_l)^8\right), \qquad r_l^2 = (x - x_0)^2 + y^2, \tag{3}$$

where δ and α are the parameters determining the level of fluid mixing inside the mixing zone and the initial radius of the local perturbation, respectively. Note that here we consider local perturbations of the density field in the form of regions of partly mixed fluid ($\delta < 1$). The interest in studying local perturbations of this kind is caused by the fact that turbulence degeneration in localized regions leads to incomplete mixing of the fluid [3]. As the functions $\varepsilon_0(r)$ and $e_0(r)$, we choose functions whose values correspond to the self-similar solution of the problem in the case of a homogeneous medium ($g = 0$) and agree with the experimental data [16].

The problem variables can be made dimensionless with the use of the velocity scale $U_0 = \sqrt{e_0(0)}$ and the length scale R (R is the initial radius of the turbulent mixing zone). As a result, in the dimensionless equations, the quantity g is replaced by the expression $4\pi^2/\mathrm{Fr}^2$, where the density Froude number (Fr) and the Brunt–Väisälä period T are determined as follows:

$$\mathrm{Fr} = \frac{U_0 T}{R}, \qquad T = \frac{2\pi}{\sqrt{ag}}, \qquad a = -\frac{1}{\rho_0}\frac{d\rho_s}{dy}, \quad y = 0.$$

The density of the unperturbed fluid is defined in the form

$$\rho_s^*(y) = \rho_0^* - \beta \tanh\,(y^*/\beta), \qquad \rho_0^* = 1/(aR) \tag{4}$$

(the dimensionless variables are marked by an asterisk). Distribution (4) corresponds to a continuous analog of a two-layer fluid, and the parameter β determines the thickness of the high-gradient interlayer of the pycnocline.

Numerical integration of the differential equations of the mathematical model was performed with the use of the stream function–vorticity variables, the method of splitting with respect to spatial variables, and orthogonal nonuniform grids refined in the vicinity of the turbulent mixing zone and the layer with a high density gradient. The numerical model was tested by conducting computations on a sequence of finite-difference grids and comparisons

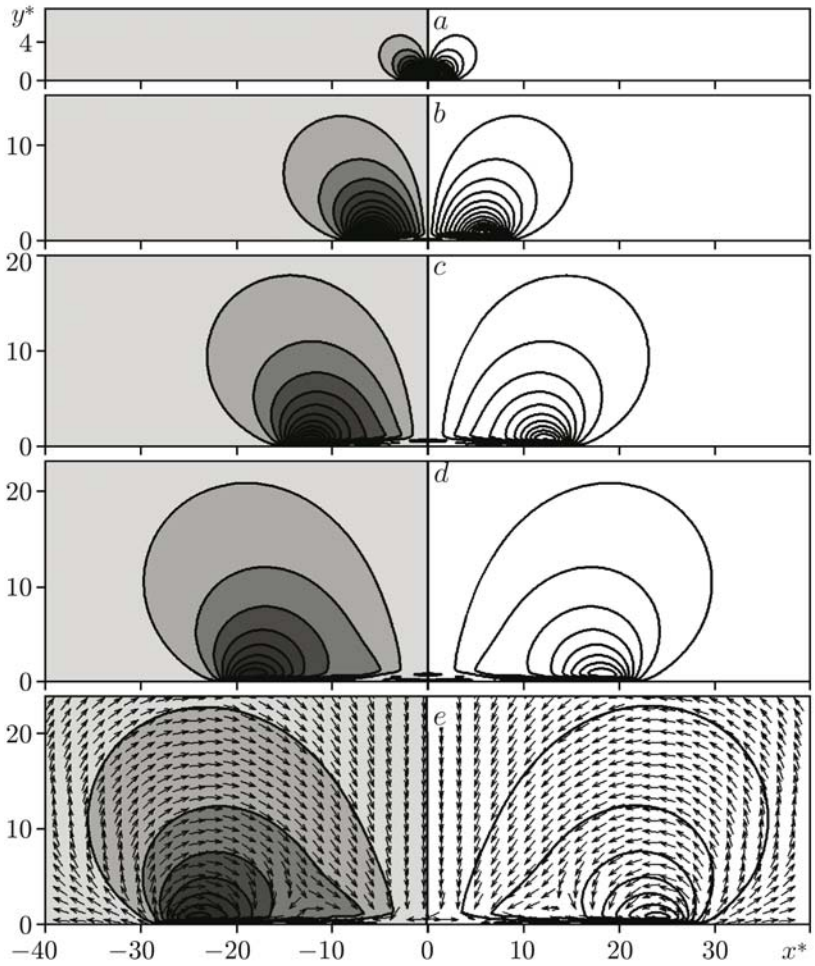

Fig. 2. Streamlines and characteristic velocity field in the problem of the dynamics of a single region of turbulent perturbations in a pycnocline at different times: the hatched area is the domain of negative values of the stream function; the arrows show the velocity field typical for this flow; the remaining notation is the same as in Fig. 1.

of the computed results with the experimental data [16] on degeneration of the characteristics of the momentumless turbulent wake in a linearly stratified medium [6, 7].

2. Interaction of a Turbulized Zone and a Local Perturbation of the Density Field in a Pycnocline. Before describing the results of numerical modeling of interaction of the flows induced by the evolution of two local perturbations (turbulent and laminar ones) in a pycnocline, we give some data on the dynamics of each flow in the absence of their interaction. It is known that these flows are characterized by the formation of a solitary internal wave in each quadrant of the plane (x, y) (see, e.g., [5, 6, 10, 11]). The convective pattern in the upper half-plane illustrates the motion of fluid particles on the right (clockwise motion) and on the left (anticlockwise motion) of the perturbation. The flow in the lower half-plane is antisymmetric. These waves propagate with time along the x axis in the opposite directions from the initial position of the local perturbation. The region of turbulent perturbations is expanded with time symmetrically relative to the coordinate axes, predominantly along the high-gradient interlayer of the pycnocline.

The results of numerical computations of the flow generated during the evolution of a single local region of turbulent perturbations in a pycnocline are presented in Figs. 1 and 2 ($\beta = 0.2$ and Fr = 18). Figure 1 shows the dynamics of the zone of turbulent perturbations $[e/e_{\max}(t) = \text{const} = 1, 0.9, \ldots, 0.1, 0.01]$ and internal waves ($\rho_0 - \langle\rho\rangle = \text{const}$). Figure 2 shows the corresponding streamlines ($\psi^* = \text{const}$ with a step of 0.0002) and the velocity field typical for this flow. At the initial stage, the turbulent perturbations inside the mixing zone make

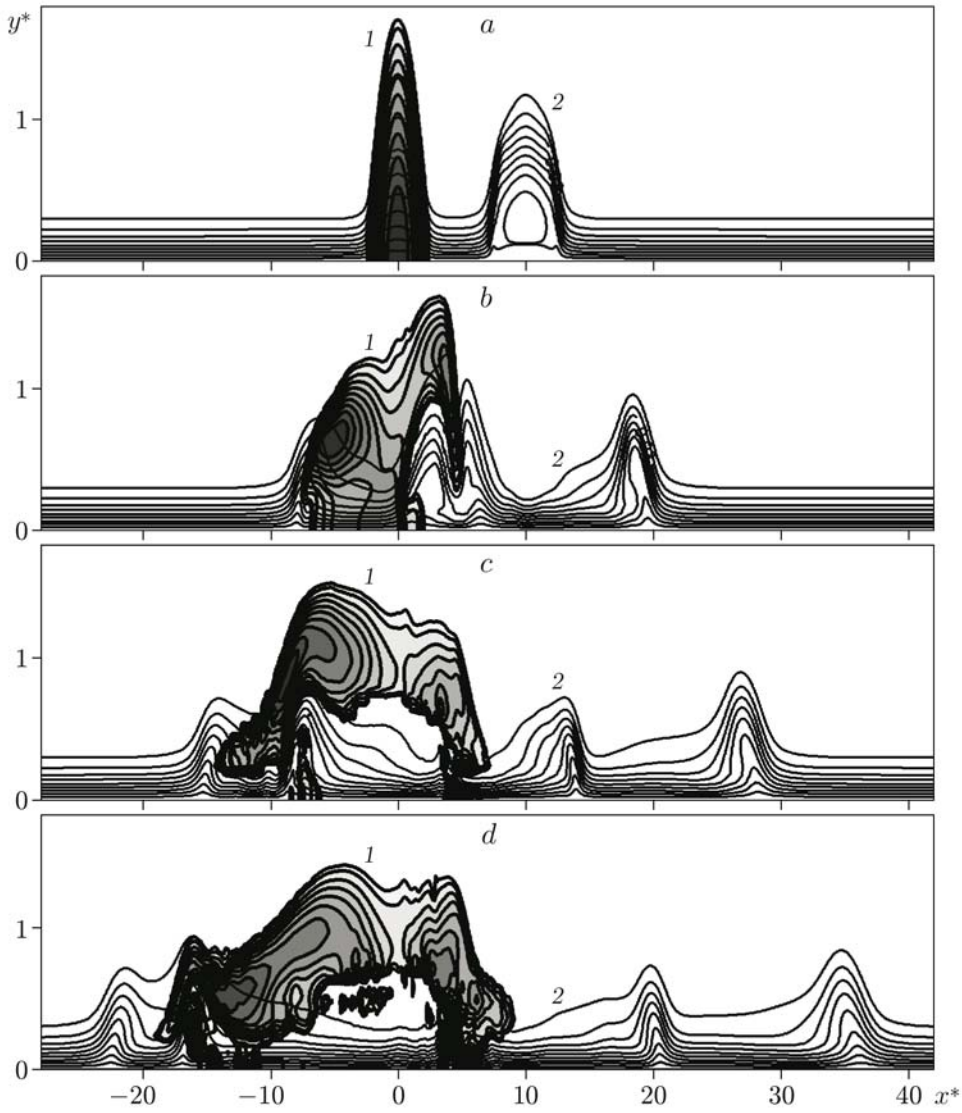

Fig. 3. Contours of the turbulence energy (1) and averaged density (2) during interaction of the localized region of turbulent perturbations and the laminar mixed region ($\alpha = 1.25$ and $\delta = 0.95$) in a pycnocline at different times: $t/T = 1$ (a), 5 (b), 10 (c), and 15 (d).

the stratified fluid particles go out from the equilibrium state. This leads to generation of solitary internal soliton-type waves whose amplitude and velocity are coupled by the Benjamin relation [17], as is seen from the analysis of numerical data.

In numerical modeling of interaction of the zone of turbulent perturbations and the local perturbation of the density field in the pycnocline, the turbulent mixing zone was located in the origin, and the center of the laminar spot of the mixed fluid was located at the point $(x_0, 0)$. In view of flow symmetry (antisymmetry), the calculations were performed in the upper half-plane with imposing appropriate conditions on the axis $y = 0$. The parameters varied in numerical experiments were the quantities α and δ determining the characteristic parameters of the local perturbation of the averaged density field and also the initial distance x_0 between the centers of the perturbations. Results for the flow with $\beta = 0.2$ and $\mathrm{Fr} = 18$ are presented below.

Figures 3 and 4 show the calculated interaction of the turbulent mixing zone and the laminar flow region, which is induced by the local perturbation (3) with the parameters $\alpha = 1.25$, $\delta = 0.95$, and $x_0^* = x_0/R = 10$. With these values of the parameters α and δ, the local perturbation of the averaged density field (3) is such that

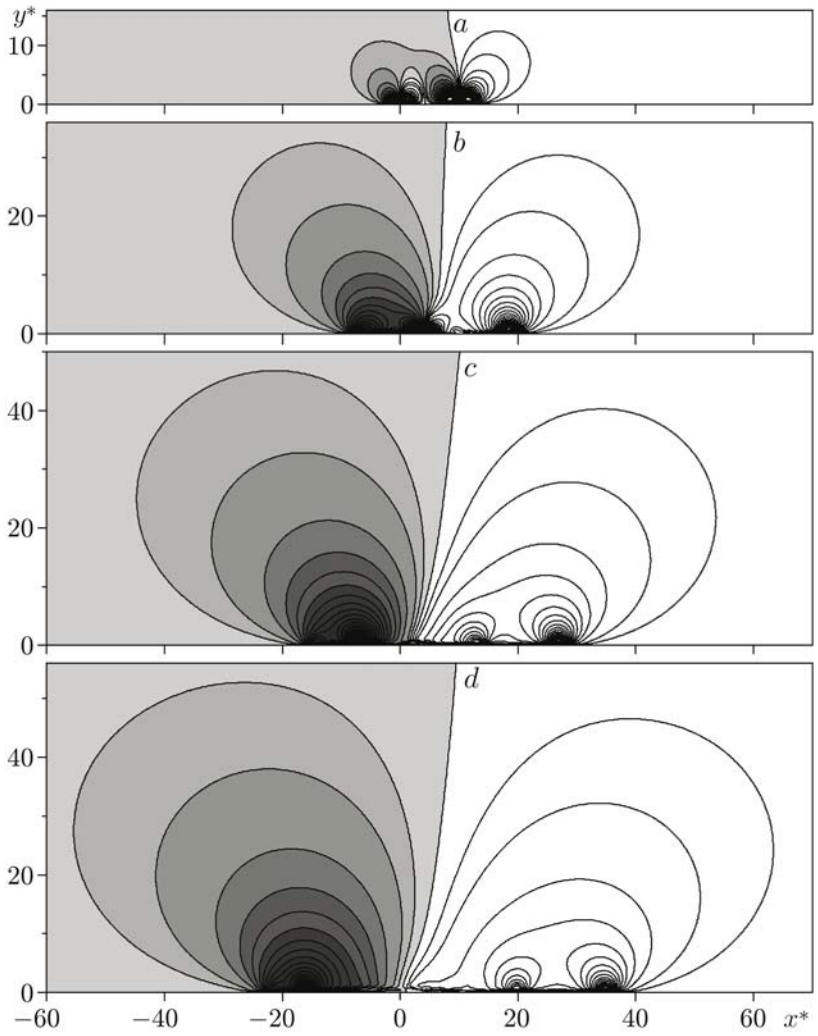

Fig. 4. Streamlines during interaction of the localized region of turbulent perturbations and the laminar mixed region ($\alpha = 1.25$ and $\delta = 0.95$) at different times: $t/T = 1$ (a), 5 (b), 10 (c), and 15 (d); the hatched area is the domain of negative values of the stream function.

the amplitude and length of the generated internal waves at high times are comparable with the corresponding parameters of internal waves generated by the region of turbulent perturbations. Figure 3 shows the contours of the turbulence energy and the corresponding contours of the averaged density at different times. It is seen that the influence of the flow induced by the local perturbation of the density field on the region of turbulent perturbations changes the structure of the turbulence spot. In particular, this change is manifested as the displacement of the turbulence zone from the horizontal axis, which is accompanied by significant deformation of the spot under the action of incoming internal waves. Numerical experiments show that the level of this deformation depends on the characteristics of the incoming solitary wave: as the parameter α in Eq. (3) is increased (which means that the total energy of this local perturbations decreases in the case of a fixed value of the mixing parameter δ), the transformation of the outer boundary of the turbulized region becomes less clearly expressed. It also follows from the analysis of Fig. 3 that there is a pair of soliton-type internal waves moving toward each other in the center of interaction. The results of calculations and their comparisons with solutions of model problems for the case without interaction show that the characteristic parameters of internal waves after their collision with specified parameters of the local perturbations change insignificantly.

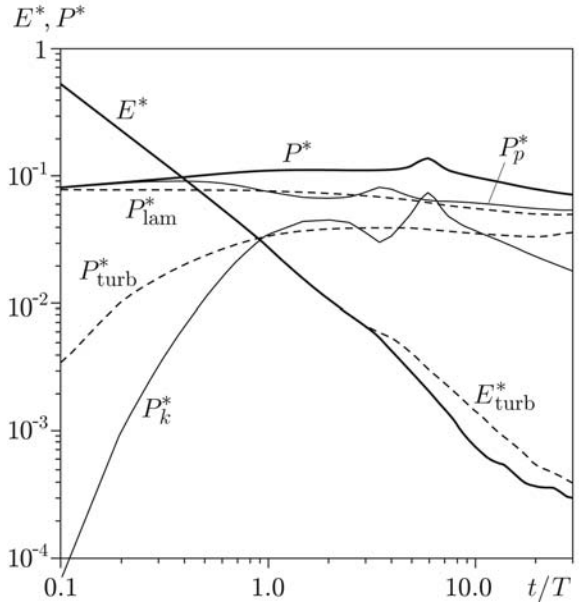

Fig. 5

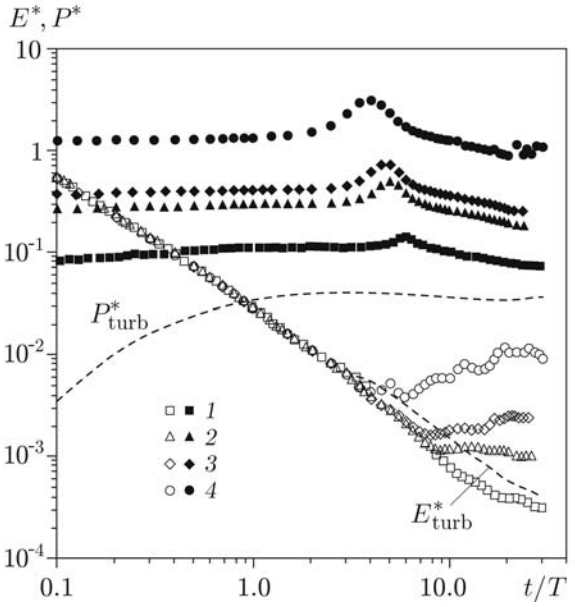

Fig. 6

Fig. 5. Time evolution of the total turbulence energy E and total energy of internal waves P: the solid curves illustrate the interaction with $\alpha = 1.25$ and $\delta = 0.95$; the dashed curves show the calculations of the turbulent and laminar local perturbations in the absence of interaction.

Fig. 6. Time evolution of the total turbulence energy E (open points) and total energy of internal waves P (filled points) during interaction of the region of turbulent perturbations and the local mixed region at $\delta = 0.95$ and $\alpha = 1.25$ (1), 0.85 (2), 0.75 (3), and 0.5 (4); the dashed curves illustrate the dynamics of the turbulized region in the absence of interaction.

The convective pattern of the flow under consideration is presented in Fig. 4, which shows the streamlines $\psi^* = \text{const}$ at different times (the step between the streamlines is 0.0002). In the domain of negative values of the stream function ψ, the fluid particles move in the clockwise direction; in the domain of positive values of ψ, they move in the anticlockwise direction. At the initial stage, the flow is characterized by the presence of two pairs of convective vortices in the opposite directions, moving to the right and left from the corresponding local perturbations along the horizontal axis. The evolution of this flow leads to a collision of the central convective vortices. When interaction is completed, the convective pattern is characterized by coalescence of the vortices having identical directions on the right and left of the interaction region.

Figures 5 and 6 show the time evolution of the total turbulence energy E and the total energy of internal waves P. The value of P can be presented as the sum of the kinetic P_k and potential P_p components of this energy:

$$E(t) = \int_0^\infty \int_{-\infty}^\infty e^* \, dx^* \, dy^*,$$

$$P(t) = \int_0^\infty \int_{-\infty}^\infty \Big(\frac{U^{*2} + V^{*2}}{2} + \frac{4\pi^2}{\text{Fr}^2} \langle \rho_1 \rangle^* y^* \Big) \, dx^* \, dy^* = P_k(t) + P_p(t).$$

Figure 5 shows the data corresponding to the solution of the problem of interaction of the turbulent spot with the local perturbation (3) at $\alpha = 1.25$ and $\delta = 0.95$. For comparison, the figure also shows the total energies P_{lam}^*, P_{turb}^*, and E_{turb}^* of the laminar and turbulent perturbations in the absence of interaction. At the stage preceding the interaction, the flow is characterized by degeneration (monotonic decrease) of the total turbulence energy E, which is identical to degeneration of E_{turb} in the dynamics of the turbulized region in the absence of interaction. The values of the total energy of internal waves P are close to constant and are only slightly higher than the

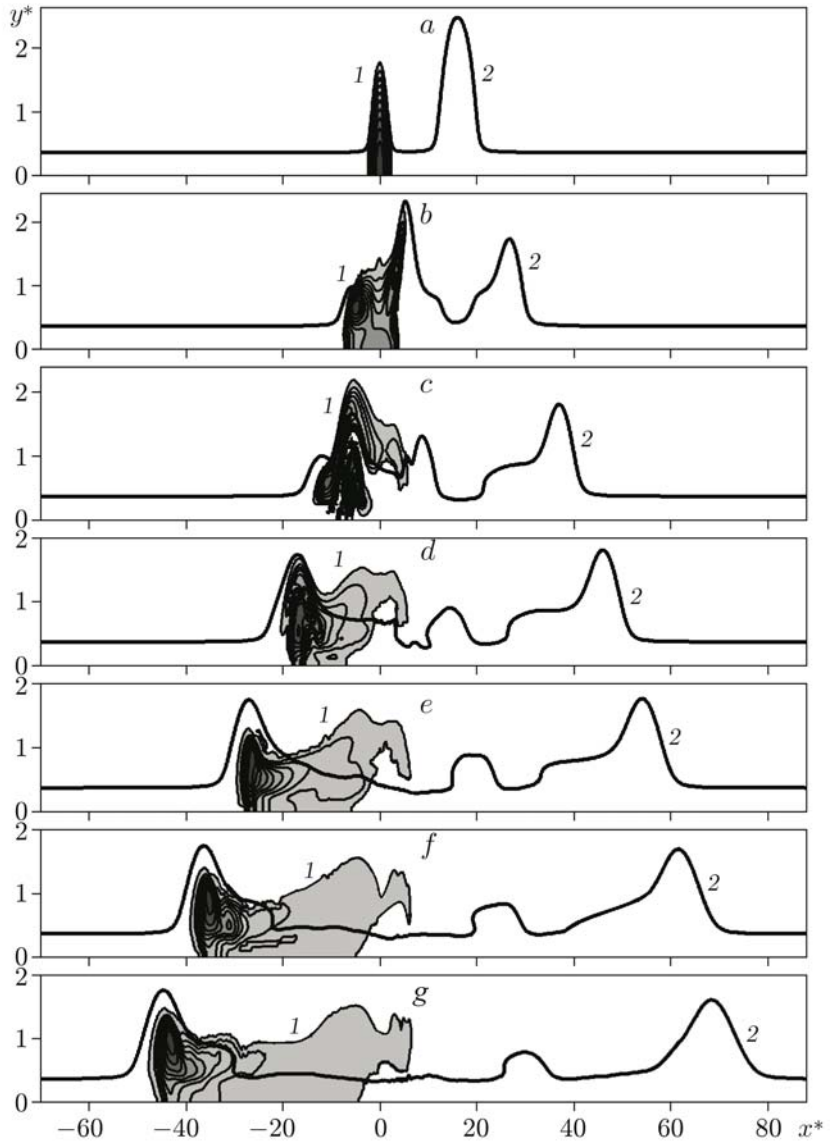

Fig. 7. Contours of the turbulence energy (1) and characteristic isoline of the averaged density (2) during interaction of the region of turbulent perturbations and the laminar mixed region ($\alpha = 0.75$ and $\delta = 0.95$) at different times: $t/T = 1$ (a), 5 (b), 10 (c), 15 (d), 20 (e), 25 (f), and 30 (g).

values of P^*_{lam} corresponding to the solution of the problem of the dynamics of a single laminar local perturbation of the density field. The process of formation of the wave pattern of the flow generated by the turbulent mixing zone is rather slow. When two convective vortices approach each other, a certain part of the kinetic energy P_k of internal waves is transformed to the potential energy P_p. In what follows, the interaction process is accompanied by an increase in the kinetic energy of internal waves, leading to an increase in the total energy of internal waves $P = P_k + P_p$, which is characterized by a somewhat faster decrease in the total energy of turbulent motion than in the case without interaction. When the interaction is completed, the total energy of internal waves is recovered to values typical for this flow before the beginning of interaction.

The initial total energy of internal waves generated by the laminar perturbation (3) was varied in numerical experiments by increasing the size of the mixed fluid region and the initial level of fluid mixing. As a result, it was found that the passage of a solitary wave having a significant amplitude and length (as compared with the characteristic size of the region of turbulent perturbations) through the turbulent spot not only deforms the region of turbulent perturbations, but also terminates degeneration of turbulence owing to the averaged motion energy (see

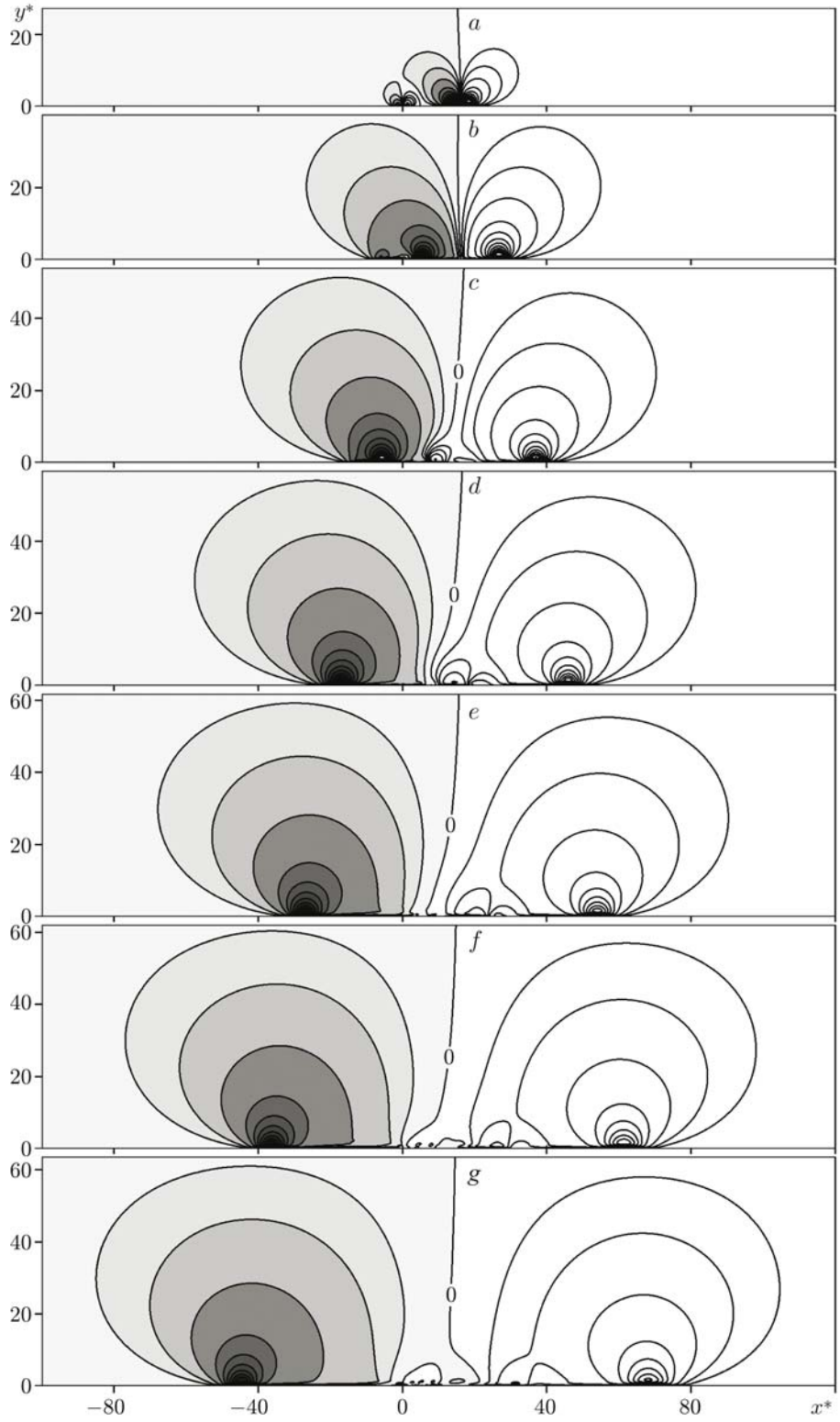

Fig. 8. Streamlines during interaction of the region of turbulent perturbations and the laminar mixed region with the parameters $\alpha = 0.75$ and $\delta = 0.95$ at different times (notation the same as in Fig. 7): the hatched area is the domain of negative values of the stream function.

Fig. 6). It is seen in Fig. 6 that an increase in the initial size of the local perturbation (decrease in the parameter α) with a fixed level of fluid mixing δ enhances the above-described effect, i.e., leads to a more significant increment of the total energy of internal waves at the stage of interaction, and the total turbulence energy reaches an almost constant value faster.

One of the situations illustrated in Fig. 6 is presented in more detail in Figs. 7 and 8, which show the flow pattern during interaction of the turbulent spot (2) with the local perturbation (3) at $\alpha = 0.75$, $\delta = 0.95$, and $x_0^* = 16$. Figure 7, which shows the contours of the turbulence energy and averaged density, illustrates the capture and transfer of the turbulent spot by the soliton-type internal wave generated by the local perturbation of the density field. It is seen in Fig. 8, which shows the corresponding convective pattern, that convective vortices generated by the laminar perturbation of the density field play the dominating role.

In a series of methodical calculations of the interaction problem, we studied the time evolution of the total turbulence energy and the total energy of internal waves as functions of the parameters of the computational grid, initial distance between the centers of the perturbations x_0, and the initial level of mixing δ. An analysis of data obtained within the framework of the mathematical model considered shows that the above-described behavior of the flow is almost independent of the parameters of the computational grid used. An increase in the initial distance between the local perturbations only delays the instant of interaction and does not change the character of the process. A decrease in the level of fluid mixing inside the local perturbation of the averaged density field with a fixed radius of this perturbation (which corresponds to a decrease in the initial amount of the total energy of internal waves) makes the total turbulence energy reach a constant value later. Methodical calculations show that the character of the flow at $\mathrm{Fr} = 36$ changes insignificantly.

It should be noted that the total turbulence energy in the time interval considered in the case without interaction decreases by more than three orders of magnitude; therefore, the time of interaction is restricted by the lifetime of the turbulent spot. The effect of deceleration of turbulence degeneration due to the incoming solitary internal wave is observed in situations where the initial energy of the laminar local perturbation of the density field is comparable with the initial total turbulence energy or is greater than the latter.

Conclusions. A numerical model of interaction of a plane turbulent mixing zone with a local perturbation of the density field in a pycnocline is constructed. The model is based on a two-dimensional system of averaged equations of hydrodynamics, which is closed by a modified $e-\varepsilon$ turbulence model. Numerical modeling of the flow is performed in a wide range of parameters of the local perturbation of the density field. It is found that the flow generated by the local perturbation of the density field can lead to appreciable generation of the turbulent energy in the turbulent mixing zone and increase the lifetime of the latter.

The authors are grateful to L. A. Ostrovskii, E. N. Pelinovskii, and L. Sh. Tsimring for discussions of the problem formulation.

This work was supported by the Russian Foundation for Basic Research (Grant No. 07-01-00363a), by the Integration Project No. 23 of the Siberian Division of the Russian Academy of Sciences, and by the Joint Integration Project No. 103 of the Siberian Division of the Russian Academy of Sciences, Far-East Division of the Russian Academy of Sciences, and Ural Division of the Russian academy of Sciences.

REFERENCES

1. J. Turner, *Buoyancy Effects in Fluids*, University Press, Cambridge (1979).
2. A. S. Monin and R. V. Ozmidov, *Ocean Turbulence* [in Russian], Gidrometeoizdat, Leningrad (1981).
3. O. F. Vasiliev, B. G. Kuznetsov, Yu. M. Lytkin, and G. G. Chernykh, "Evolution of the turbulized fluid region in a stratified medium," *Izv. Akad. Nauk SSSR, Mekh. Zhidk. Gaza*, No. 3, 45–52 (1974).
4. O. F. Vasiliev, B. G. Kuznetsov, Yu. M. Lytkin, and G. G. Chernykh, "Development of the turbulent mixing zone in a stratified medium," in: *Heat Transfer and Turbulent Buoyant Convection*, Proc. of the Int. Seminar (Dubrovnic, Yugoslavia, August 30–September 4, 1976), Vol. 2, Hemisphere, Washington (1977), pp. 123–136.
5. T. W. Kao and H. P. Pao, "Wake collapse in the thermocline and internal solitary waves," *J. Fluid Mech.*, **97**, No. 1, 115–127 (1980).
6. O. F. Voropayeva and G. G. Chernykh, "Evolution of the turbulent mixing zone in a nonlinearly stratified fluid," *Model. Mekh.*, **3**, No. 5, 3–29 (1989).

7. Yu. D. Chashechkin, G. G. Chernykh, and O. F. Voropayeva, "The propagation of a passive admixture from a local instantaneous source in a turbulent mixing zone," *Int. J. Comput. Fluid Dyn.*, **19**, No. 7, 517–529 (2005).
8. G. G. Chernykh and O. F. Voropayeva, "Numerical simulation of turbulent mixing zone in stable stratified medium using second order mathematical models," *Russ. J. Numer. Anal. Math. Model.*, **24**, No. 1, 15–30 (2009).
9. V. A. Gushchin, "Method of splitting for problems of inhomogeneous fluid dynamics," *Zh. Vychisl. Mat. Mat. Fiz.*, **21**, No. 4, 1003–1017 (1981).
10. A. N. Zudin and G. G. Chernykh, "Effect of viscosity on the dynamics of a local perturbation of the density field in the pycnocline," *Model. Mekh.*, **4**, No. 3, 71–78 (1990).
11. V. S. Maderich, G. J. E. van Heijst, and A. Brandt, "Laboratory experiments on intrusive flows and internal waves in a pycnocline," *J. Fluid Mech.*, **432**, 285–322 (2001).
12. G. G. Chernykh and A. N. Zudin, "Linear and nonlinear numerical models of local density perturbation dynamics in a stable stratified medium," *Russ. J. Numer. Anal. Math. Model.*, **20**, No. 6, 513–534 (2005).
13. T. O. Abramyan and A. M. Kudin, "Laboratory study of interaction of mixed fluid spots spreading in a stratified medium," *Izv. Akad. Nauk SSSR, Fiz. Atmos. Okeana*, **19**, No. 8, 888–891 (1983).
14. H. Honji, N. Matsunaga, Y. Sugihara, and K. Sakai, "Experimental observation of internal symmetric solitary waves in a two-layer fluid," *Fluid Dyn. Res.*, **15**, 89–102 (1995).
15. W. Rodi, "Examples of calculation methods for flow and mixing in stratified fluids," *J. Geophys. Res.*, **92**, 5305–5328 (1987).
16. J. T. Lin and Y. H. Pao, "Wakes in stratified fluids," *Annu. Rev. Fluid Mech.*, **11**, 317–336 (1979).
17. T. B. Benjamin, "Internal waves of permanent form in fluids of great depth," *J. Fluid Mech.*, **29**, No. 3, 559–592 (1967).